Characterising gradient artefacts in simultaneous EEG/fMRI through physical modelling

W. X. Yan[1], K. J. Mullinger[1], M. J. Brookes[1], and R. W. Bowtell[1]

[1]Sir Peter Mansfield Magnetic Resonance Centre, School of Physics and Astronomy, University of Nottingham, Nottingham, Nottinghamshire, United Kingdom

Introduction

Functional magnetic resonance imaging (fMRI) generates large artefacts in concurrent electroencephalography (EEG) recordings that can significantly compromise EEG data quality (1-2). While much effort has been applied in studying the temporal variation of the artefact waveforms produced by time-varying magnetic field gradients (2-3), the spatial variation of the artefact voltage across EEG leads has not previously been investigated in any depth. The aim of this work is to develop an improved understanding of the spatial characteristics of the gradient artefacts and the mechanism which underlies their generation. The resulting insights can be used to reduce the magnitude of artefacts at source and improve the efficacy of artefact correction.

Theory and Methods

In this work, we have developed analytical expressions for the artefact voltage assuming a simple head model and EEG lead geometry. We have also implemented numerical calculations based on the actual lead paths. The results have been compared with experimental measurements made on simple phantoms and the human head.

$$V = \int_B^A \frac{\partial \mathbf{A}}{\partial t}\cdot \mathbf{dl} - \int_B^C \frac{\partial \mathbf{A}}{\partial t}\cdot \mathbf{dl} + \Phi_A - \Phi_C \quad [1]$$

$$V = -\frac{1}{6}\dot{G}\, a^2 \sin\phi\left(2a\sin\theta + 3z_0\theta\right) \quad [2]$$

Analytical and Numerical: Previously it has been assumed that gradient artefacts can be modelled in terms of the time-varying magnetic flux induced in wire loops formed by the leads and head (4). This is incorrect as it neglects the fact that the head is a volume conductor so that there is not a single current path between two electrodes (5). To derive the correct form of the artefact voltage, we consider two contributions: (i) the line integral of the electric field induced in the leads (which depends on the temporal derivative of the vector potential, **A**) and (ii) the scalar potential, Φ, resulting from the redistribution of charges in the volume conductor. In the scenario described by Figure 1, the sum of these two components is given by Eq. [1], where the 'data' electrode is at point 'A', the 'reference' electrode at point 'C', and the leads meet at the cable bundle at point 'B'. In the analytic model, we assumed that the head could be represented as a uniform spherical conductor and that the leads ran along the meridians of the sphere from the cable bundle at the north pole of the sphere to the electrode. We also assumed the induced voltages in the data and reference lead segments along the cable bundle are equal and opposite due to its small cross section, and voltages induced in the cables running between the EEG cap and the amplifiers are therefore neglected. Analytic expressions for the artefact voltages were generated from Eq. [1] by using the vector potentials corresponding to pure longitudinal and transverse gradients and standard methods to solve for the potential in the sphere (6). The effect of changing the head position with respect to the gradients was accommodated by rotating and translating the vector potentials. In the numerical calculations, the line integrals of Eq. [1] were calculated using the actual lead paths and electrode positions obtained by digitizing the paths of the leads on the phantom or head using a Polhemus Isotrak. For these calculations, the scalar potential contribution was evaluated based on the best fitting sphere to the head or phantom, onto which the electrodes were then projected.

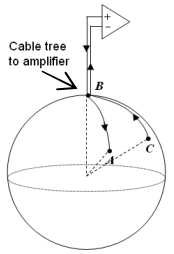

Figure 1: *Schematic of the electrode paths in EEG.*

Experimental: Artefact voltages were initially measured using a 19 cm diameter, saline loaded spherical agar phantom (7) fitted with a 32-electrode MR-compatible EEG cap (EasyCap, Herrsching). Vitamin E capsules were used to mark fiducial points on the phantom, allowing alignment of the scanner and phantom co-ordinates for later analysis. A BrainAmp MR-plus EEG amplifier (with a 0.016-1000Hz frequency range) and Brain Vision Recorder software (Brain Products, Munich) were used for data recording. Artefacts were generated on a 3T Philips Achieva MR scanner specially programmed to generate single gradient pulses with a controlled rate of gradient field variation, $\dot{G}$ =2 $Tm^{-1}s^{-1}$. The phantom was positioned at the scanner's isocentre and EEG recordings were made with gradient pulses applied in the Anterior-Posterior (AP), Right-Left (RL) and Foot-Head (FH) directions. The bed was then moved 3 cm towards the feet and the measurements repeated. Similar measurements were also made on a human head. The EEG data were analysed using Matlab and Brain Vision Analyzer software (Brain Products, Munich). In the following, we focus on the results obtained when transverse gradients (LR and AP) were applied.

Results and Discussion

Analytical: Eq. [2] describes the artefact generated by a transverse gradient applied in the *x*-direction (LR) when the reference electrode lies at the pole and the sphere's north-south axis is aligned with the main magnetic field direction. Here a is the sphere's radius, while θ and ϕ describe the electrode position on its surface, and z_o characterises the axial offset of the sphere from the scanner's isocentre. This expression indicates that the artefact voltage: (i) is proportional to $\dot{G}$, as expected; (ii) increases with the radius of the sphere, implying gradient artefacts scale with head size; (iii) shows a predominately AP variation for a gradient applied in the LR direction; (iv) depends on the offset z_0, so adjustment of the axial position of the head can potentially be used to reduce the gradient artefact voltages. A similar expression for the case of a gradient applied in the *y*-direction (AP) can be generated by replacing $\sin\phi$ with $\cos\phi$ in Eq. [2], producing an artefact voltage that varies predominately in the LR direction.

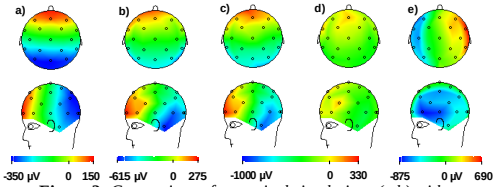

Figure 2: *Comparison of numerical simulations (a,b) with experimental measurements (c,d,e).*

Numerical and Experimental: Figure 2 shows numerically simulated (Fig. 2a-b) and experimentally measured (Fig. 2c-e) artefact voltage patterns for the spherical phantom exposed to a time-varying *x*-gradient. Although the general form of the simulated pattern for simple meridional lead paths (Fig. 2a) is similar to measurements on the centred spherical phantom (Fig. 2c), better agreement is achieved when the digitised wire-paths are used in the numerical calculation (Fig. 2b). This is evident from the correlation coefficient of measured and simulated artefact voltages across electrodes, which takes a value of 0.90 for the meridional wire-paths versus a value of 0.98 for the digitized, actual wirepaths. Figure 2d shows that moving the phantom axially by 3 cm towards the feet reduces the magnitude of the experimentally measured artefact, yielding a 49% reduction in the RMS voltage. This reduction, which is also seen in numerical simulations and measurements with other gradient orientations, is in agreement with the prediction of the analytical model (Eq. [2]). Figure 2e shows the artefact voltages measured from the phantom when the gradient is applied in the AP direction. This confirms the model's prediction that the artefact pattern varies predominantly in the LR direction for an AP gradient. Figure 3 shows numerical and measured artefact voltage maps for the human head when the gradient was applied in the LR direction. A correlation coefficient of 0.78 was calculated for these data, indicating good agreement between simulation and measurement. Moving the subject axially by 3 cm in the direction of the feet produced a 53% reduction in the RMS artefact voltage. Small inconsistencies in the amplitude of the measured artefact compared with the numerical results are likely to be due to the finite cross section of the cable tree which means that some artefact arises from flux changes linked by wires running from the EEG cap to the amplifiers.

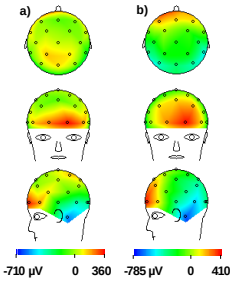

Figure 3: *Numerical (a) vs. experimental (b) data for head*

Conclusions

Starting from basic physical principles, we have modelled the spatial distribution of the gradient artefacts in EEG-fMRI for both a phantom and human head with a high degree of accuracy. The results show that axial adjustment of head position can be used to reduce the magnitude of induced artefacts. The approach described here could be useful for identifying new EEG cap designs that yield smaller gradient artefact voltages. In addition, the accuracy of the modelling along with the ability to evaluate gradient artefacts for any head orientation should facilitate the development of improved artefact correction algorithms that incorporate motion tracking of the subject and selective filtering based on calculated spatial artefact templates.

References [1] Allen *et al.* Neuroimage 8**:**229,1998 **[2]** Allen *et al*. Neuroimage 12:230,2000 **[3]** Mandelkow *et al* Neuroimage 32**:**1120 **[4]** Masterton *et al* Neuroimage 37:202, 2007 **[5]** Glover and Bowtell PMB 52:5119, 2007 **[6]** Bencsik *et al* PMB 47:557**,** 2002 **[7]** Geirsdottir *et al* Proc. 16th ISMRM 2008 #3626